JOURNAL OF THEORETICAL
AND APPLIED MECHANICS
43, 2, pp. 309-325, Warsaw 2005

NUMERICAL AND EXPERIMENTAL ANALYSIS OF PRELIMINARY STRESS, LIMITING LOAD CAPACITY AND FATIGUE LIFE OF BLIND RIVETED JOINTS[1]

LUCJAN WITEK

Faculty of Mechanical Engineering and Aeronautics, Rzeszów University of Technology
e-mail: lwitek@prz.rzeszow.pl

This paper presents results of numerical static and fatigue calculations as well as experimental investigations of the lap blind riveted joint. The first port of this study is concerned with numerical analysis of phenomena occurring in the process of blind riveting. In the results of nonlinear computation performed for a joint with one rivet, the initial stress distribution, plot of the riveting force in function of the rivet core displacement and plastic strain distribution were obtained. In the next step, the riveted joint with a defined initial stress state was subjected to shear. The analysis was additionally made for a few models with different numbers of finite elements. The obtained numerical results: load-displacement characteristics and the limiting load capacity for the considered riveted joint were validated in experimental investigation. The next part of the paper presents results of numerical fatigue analysis performed for a riveted joint loaded by a cyclic force. In that computation, the number of cycles to total damage of main joint components was estimated.

Key words: riveted joint, initial stress, limiting load capacity

1. Introduction

Riveted joints still play a major role in assembling technology of thin-walled structures. The main advantage of this type of joints is basically the repeatability of strength and fatigue properties. Riveted joints have also certain disadvantages, e.g. large labour consumption, however they are still widely

[1]The work won the 3-rd prize of the Professor Jan Szmelter all-country conquest for the best paper on engineering mechanics.

used in the aviation industry. In the manufacturing process of many airframe components as wing, flaps, aileron or tail units, special blind rivets which enable riveting closed sections of structures must be used. The technological process of blind riveting is not very complicated. Moreover, low cost of blind rivets caused that nowadays this kind of rivets is commonly used not only in the aviation but in other branches of industry.

For many years, several studies concerned with the increase of the strength and fatigue life of riveted joints have been performed. In the past, these investigations were mainly based on experimental tests because analytical description of phenomena occurring in riveting or shear processes are very complex. In experimental tests, different techniques such as interferometry, photoelasticity or tensometric strain measurment were used. Results of several latest investigations devoted to the problem of maximum load, stress distribution or fatigue life of riveted joints were described by Fitzgerald and Cohen (1994), DiBattista *et al.* (1998), Lucas *et al.* (2000), Witek (2000, 2002), Terada (2001), Galatolo and Nillson (2001), Urban (2003), Kelly and Costello (2004).

Rapid development of many numerical methods in connection with contemporary multiprocessor supercomputers with huge computational power caused that many nonlinear engineering problems such as contact and plasticity can be solved numerically. Nowadays, many commercial programs have the possibility of simulating nonlinear phenomena occurring in riveting or loading processes of joints. In the study by Fung and Smart (1997), the authors estimated the initial stress and stain occurred in a riveted lap joint. In this paper, the influence of friction and thickness of connected sheets on the preliminary stress distribution are additionally examined. The problem of numerical evaluation of the limiting load capacity of sheared riveted joints is also described by Langrand *et al.* (1999, 2000, 2002). Deng and Hutchinson (1998) described numerical investigation of a phenomenon occurring in the riveting process with the use of the classical solid rivet. Using nonlinear FE analysis, the authors specified separated phases of riveting concerned with variability of the riveting force. An interesting study is the work by Al-Emrani and Kliger (2003) in which a riveted bracket of a railway bridge was investigated. In that work, the authors considered a detailed FE model of a joint consisting of 10 rivets.

A similar problem of numerical analysis of stress, strain and fatigue life of riveted joints was also described by: Xiong (1999), Witek (1999, 2000, 2001, 2002), Liao *et al.* (2001), Neves *et al.* (2001), Liu and Sawa (2001), Karaoglu and Kuralay (2002).

In this study, attention is mainly paid to mechanical phenomena occurring in the process of blind riveting, loading of joints and their durability in fatigue

2. Analysis of initial stress forming in the process of blind riveting

The subject of investigation is a separated fragment of a single-riveted lap joint, consisting of one blind rivet (diameter 3.2 mm) and two sheets (upper and lower) with thickness of 1 mm and width of 20 mm. Due to complexity of the problem (nonlinear material, contact and nonlinear analysis) the investigation is limited to a joint consisting of one rivet only. To create a model of the joint and define loads and boundary conditions, the program MSC-Patran 2000 has been used.

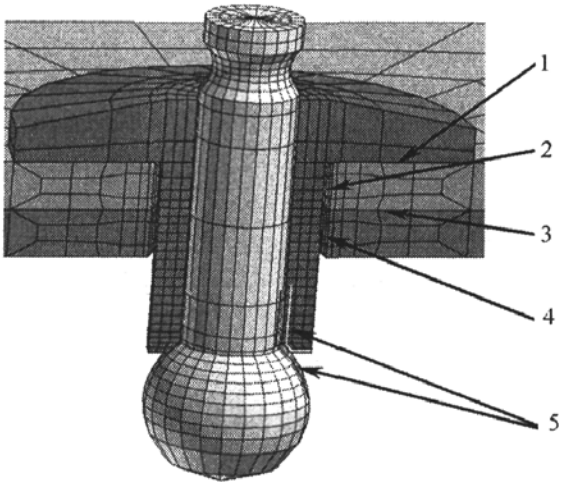

Fig. 1. The first model of joint components before riveting with defined contact surfaces

Figure 1 shows the first numerical model with distinguished components of the joint before riveting. In this figure, 5 pairs of surfaces which can potentially be in contact during the riveting process are additionally shown. In pairs 1-4, the contact with small sliding is assumed (16). The contact with small sliding can be used for modeling contact phenomena unless displacement of one surface along the second is smaller than the size of the used finite element.

In 5-th pair, contact with large sliding is additionally defined. The friction coefficient between the contact surfaces is set as 0.1.

In the second variant of the model, the core of the blind rivet with a spherical tip is replaced by a fragment of an undeformed spherical surface. The main advantage of such solution is the possibility of mesh concentration in the vicinity of high plastic strain areas of the model occurring in riveting and shearing processes at the same size of the numerical task. The shown in Fig. 2 finite element model consists of 7664 solid HEX-8 elements. Moreover, models of joints with 2916 and 4046 elements are also created. The results presented in Fig. 4 - Fig. 11 concerned the second variant of the model with dense mesh (7664 elements). In the analysis, the top part of the rivet and tips of sheets were fixed with a displacement vector of 1.3 mm applied to the spherical surface. The preliminary analysis conducted for the displacement vector of 2 mm was stopped due to numerical problems concerned with large plastic strain in the last phase of riveting at the time step of 0.613 (for core displacement of about 1.22 mm). For this reason, the value of the core displacement vector was reduced to 1.3 mm.

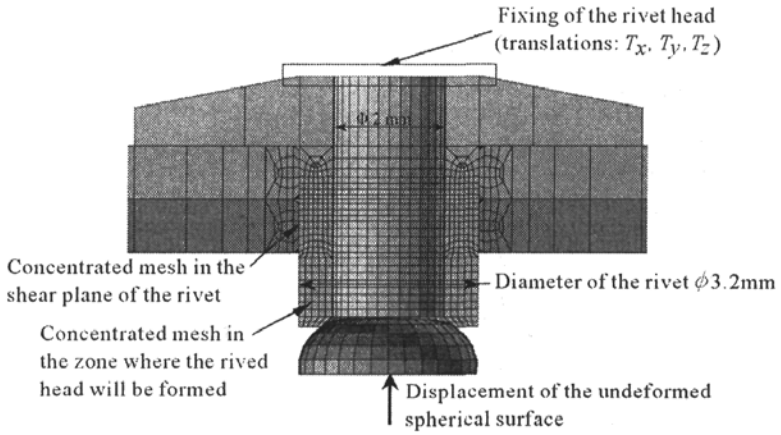

Fig. 2. The second model of the joint with defined load and boundary conditions for the riveting process

The material of lower and upper sheets was defined as linear-elastic with Young's modulus 7200 MPa and Poisson's ratio 0.3 (mat. PA-7). A discrete characteristic of the elasto-plastic rivet material with isotropic hardening, presented in Fig. 3b on the basis of the real stress-plastic strain characteristic (Fig. 3a) for the alloy PA-20 (Polish Standard PN-79/H82160), was defined. In numerical calculations, the nonlinear Newton-Raphson procedure (18) and theory of large displacements, implemented into the MSC-Advanced FEA so-

lver were used. In the Newton-Raphson method, a displacement vector of 1.3 mm on a small portion of the load was first divided. In consecutive steps of nonlinear analysis, these mentioned parts of the load were added to the load from the previous step. The values of riveting and shearing forces for successive steps of analysis are marked by circles on the plots presented in Fig. 6 and Fig. 12. For all presented results, Megapascal (MPa) units for the description of the fields of stresses are used.

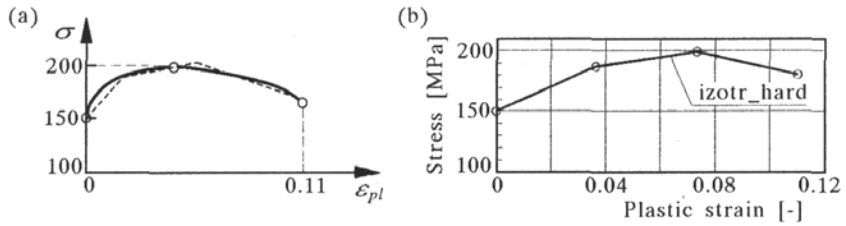

Fig. 3. A plot of stress vs. plastic strain for the alloy PA-20 (a) and the discrete characteristic of this material used in computation (b)

Figures 4 and 5 show plastic strain and Von Mises stress distribution for the joint in early and final phases of riveting.

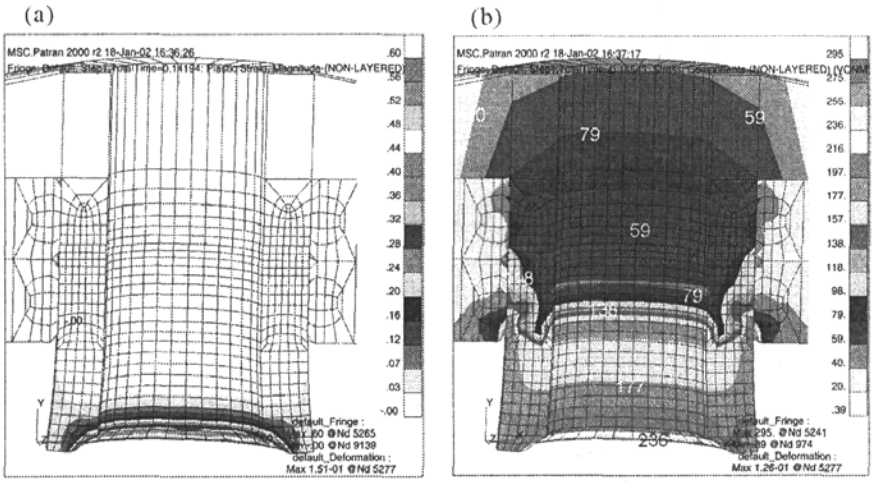

Fig. 4. Plastic strain (a) and Von Mises stress (b) distribution in an early stage of riveting (riveting force – 450 N)

As can be seen in Fig. 4, in the first step of riveting, the plastic strain area in the vicinity of the bottom part of the rivet is located. In this phase, the spherical tip of the core comes into contact with the rivet and rapid growth of

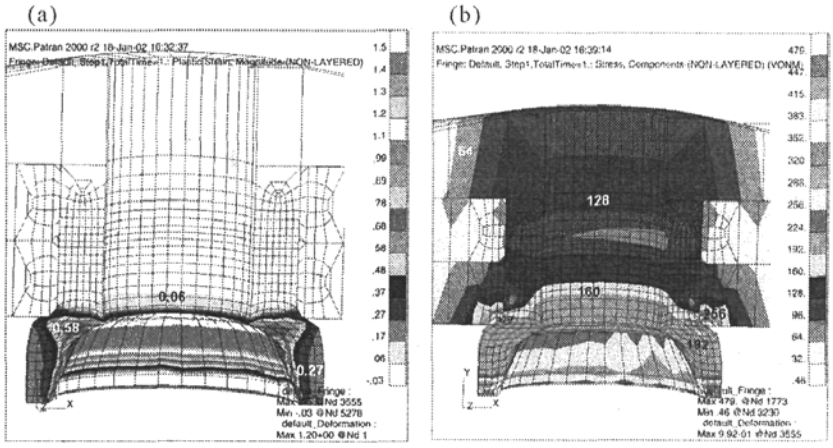

Fig. 5. Plastic strain (a) and Von Mises stress (b) distribution in the final phase of riveting (riveting force – 1280 N)

the riveting force shown in Fig. 6 is observed. In the next stage of the riveting, the bottom part of the rivet expands, and a formed rivet head for slowly increasing force is created.

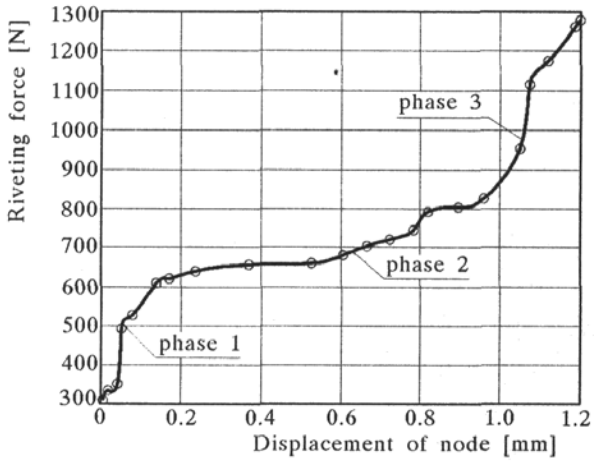

Fig. 6. A plot of the riveting force in function of rivet core displacement; phase 1 – entry of the spherical tip of the core in contact with the rivet, phase 2 – creation of the formed rivet head, phase 3 – compression of the sheet pack and breaking of the core

The last phase of riveting begins when the successive rapid growth of the force in the rivet core occurs. In this stage, the pack of sheets is compressed. After that, the rivet core is broken but residual stresses in the joint remain,

which can have significant influence on the limiting load capacity of the sheared joint. These stresses are also named as initial or preliminary.

The initial stress distribution (after breaking of the core) in the riveted joints is presented in Fig. 7. The value of the force needed to break the core was estimated on the base of information on the cross section area and strength of the core material. The zone of the maximum residual Von Mises stress (150-204 MPa) is located in the bottom part of the rivet, where the formed rivet head was created. In the shearing section of the rivet, the stress ranges between 37-56 MPa.

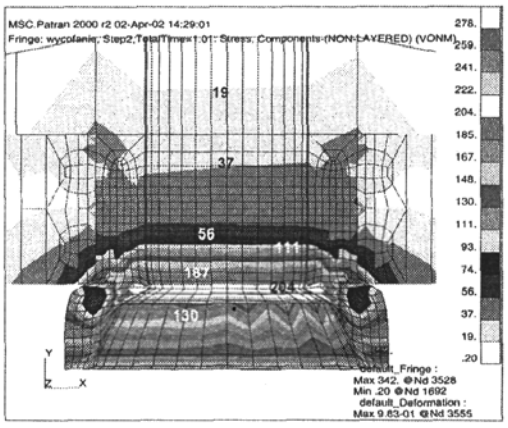

Fig. 7. Residual Von Mises stress distribution in the joint after the process of riveting

3. Numerical analysis of the limiting load capacity of the blind riveted lap joint

In the next step of numerical analysis, the riveted joint with the defined initial stress (see Fig. 7) was subjected to shear. The load and boundary conditions used in the shearing process are shown in Fig. 8. In this analysis, the end part of the lower sheet was restrained, while to the edge of the upper sheet a 1 mm displacement vector was applied. To model the mechanical interface of adjacent surfaces of the rivet and sheets, 4 pairs of contact surfaces (presented in Fig. 1) with small sliding and friction coefficients of 0.1 were defined. The 5-th contact pair in the shearing analysis was neglected because the core of the rivet is lost after riveting.

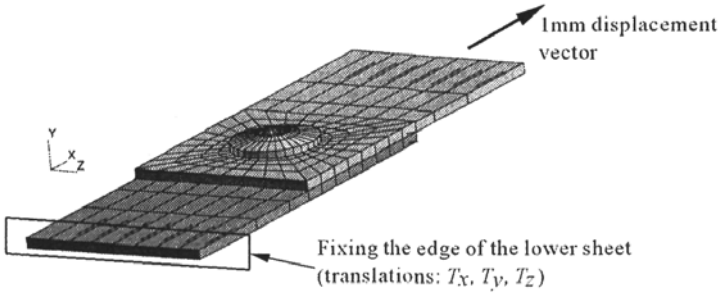

Fig. 8. Load and boundary conditions for a numerical model of the joint in the rivet shear process

Figure 9 shows Von Mises stress distribution displayed on a deformed model of the joint in an early and final phase of shear. As can be seen in this figure, in the preliminary step, for the shearing force of 300 N (Fig. 9a), the initial stress located in the bottom part of the rivet is dominant. For a larger load (600 N), the stress in the sheet on the corner of hole increases to value of 407 MPa (Fig. 9b).

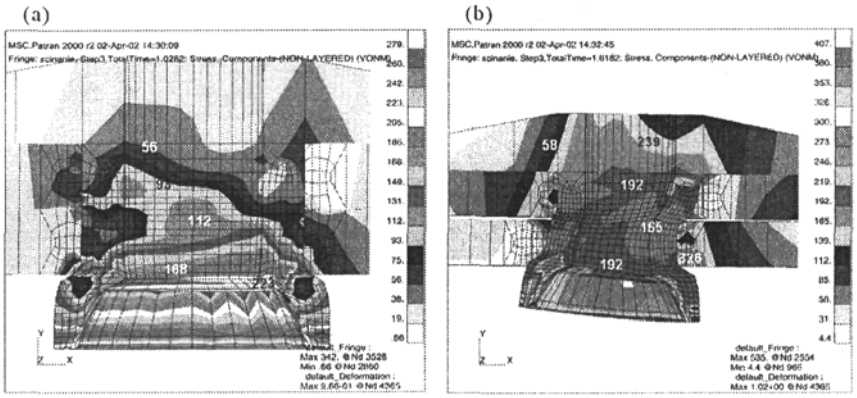

Fig. 9. Von Mises stress distribution for the joint in the initial (a) and last(b) phase of shearing

Figure 10 presents the plastic strain distribution (a) and a view of the deformed rivet (b) in the last step of analysis. The zone of maximum plastic strain occurs in the bottom part of the rivet, where the rivet head was earlier formed. Additionally, during loading of the joint, in the shear section of the rivet (in the plane of sheets contact) there appears a new plastic strain zone. Values of plastic and elastic strain along the vertical line on the external surface of the rivet (line A-B) are presented in Fig. 11. Figures 10 and 11 show that the main mechanism of rivet damage is the large plastic strain occurring in the

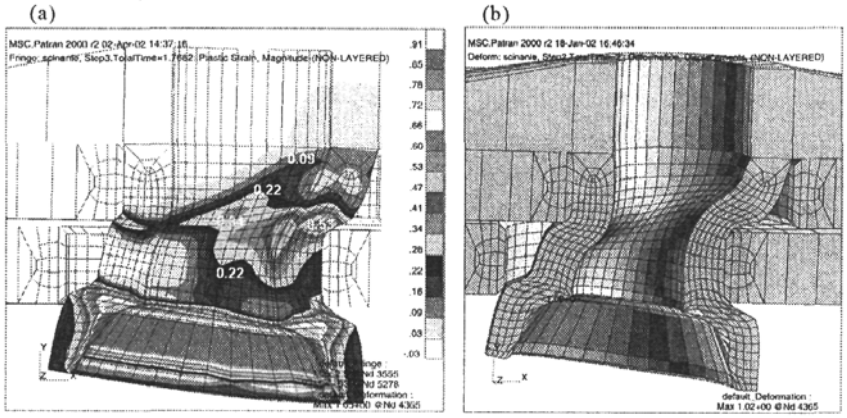

Fig. 10. Plastic strain distribution (a) and view of the deformed rivet (b) in a highly loaded joint at in the find step of analysis

shear section of the rivet. Failure of the joint occurs when the plastic strain in the shear section of the rivet achieves a certain limited value (concerned with coherence forces of the material).

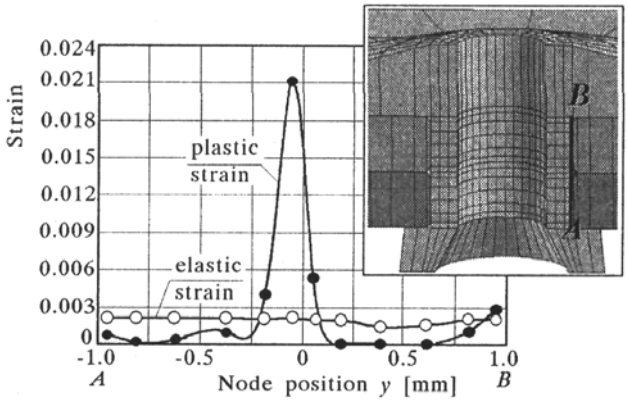

Fig. 11. Magnitude of plastic and elastic strain along the vertical line on the external surface of the rivet (line A-B) in the preliminary phase of shearing

The program MSC-Patran enables tracking many parameters during nonlinear analysis for a selected node of the model. The numerical load-displacement characteristic of the riveted joint presented in Fig. 12 was obtained through tracking displacements and forces in the node, where a concentrated load was applied (node in the axis of symmetry of sheets). As seen in this figure, the maximum loads for 3 analyzed models with different numbers of elements are very similar (580-620 N) with a difference lower than 8%.

Taking into account also the time of computation (model with 7664 elements – 100 hours; model with 2916 elements – 10 hours), analysis of the model with dense mesh was not very effective in this case. The point of rivet failure is not visible in Fig. 12 because the used numerical model of the material does not have any implemented damage criteria. The marked dashed line, shown in Fig. 15, has been found on the base of the real load-displacement characteristic of the joint. This line represents the phase of rivet damage.

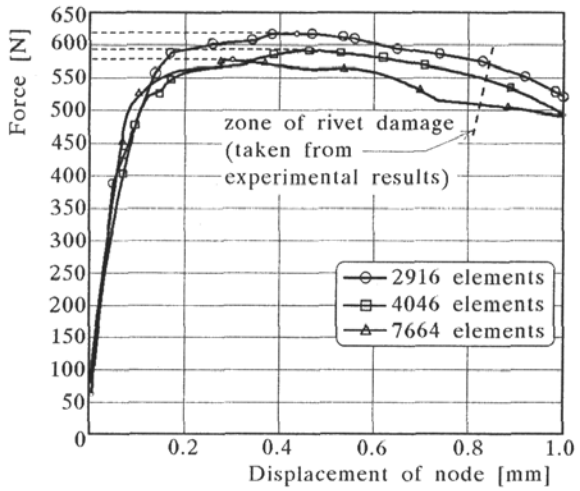

Fig. 12. Numerical load-displacement characteristics for joints with different numbers of elements

4. Experimental verification of the limiting load capacity of a blind riveted lap joint

The results obtained from numerical calculations, were then validated by experimental investigation. In the investigations, the specimens (Fig. 13) consisting of one blind rivet (manufactured out of PA-20 alloy) and 2 sheets (manufactured out of PA-7 alloy) were subjected to shear.

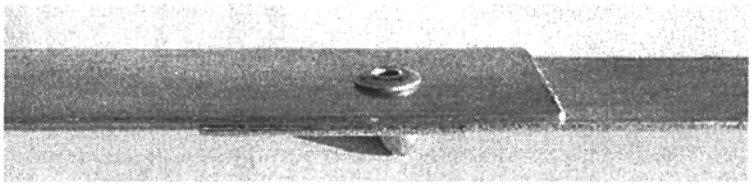

Fig. 13. View of the specimen used in experimental tests

The experimental investigation was carried out with the use of a testing machine shown in Fig. 14. The machine was characterized by the operating range of 0-1000 N and a mechanical control of the load.

Figure 15 presents an experimental shear force-displacement characteristic for a riveted joint. As it is seen in this graph, the maximum force (real limiting load capacity) of the joint is approximately 705 N. The specimen was damaged by upper sheet displacement of 0.8 mm.

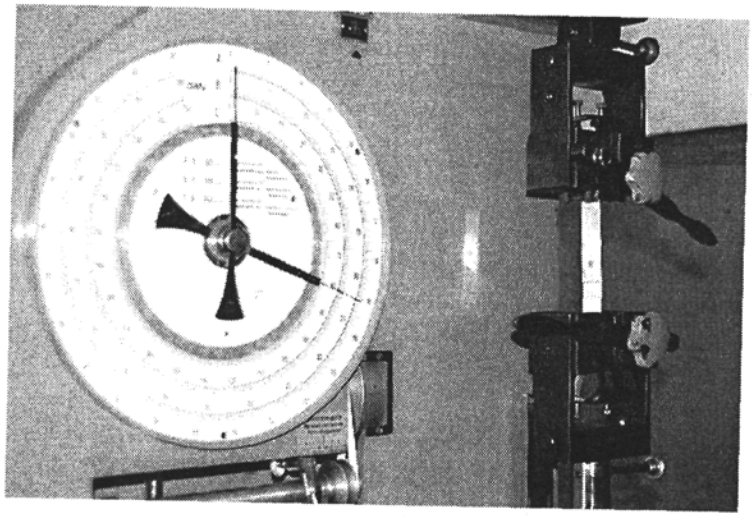

Fig. 14. A mechanical testing machine used in the experimental investigation of riveted joints

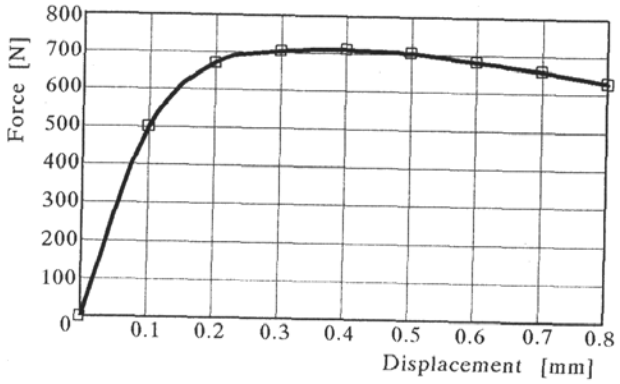

Fig. 15. The experimental load-displacement characteristic for the sheared riveted joint

By comparison of the experimental (Fig. 15) and numerical (Fig. 12) characteristics, it is easily seen that the course of both curves is similar. The maximum force obtained in the experiment was higher than the numerical limiting load value by about 12%. This difference was probably caused by incompatibility between the numerical characteristic of the rivet material taken from Standard PN-79/H82160 and the real characteristic of the blind rivet alloy.

A view of damaged rivet in experimental test is shown in Fig. 16. As can be seen in this figure, the first phase of the rivet damage process is stable plastic shearing in the plane of sheets contact. This zone is visible on the left smooth zone of fracture. The total failure of the joint occurs when the plastic strain in the shear plane of the rivet achieves a certain limiting value, concerned with the coherence forces of the material. The brittle fracture zone is visible in the right area of the damaged rivet as a rough surface. Different yield points of used joint alloys (rivet: $R_e = 200\,\text{MPa}$; sheets: $R_e = 370\,\text{MPa}$) caused that the significant plastic strain areas were not observed in the vicinity of holes in the sheets. Conclusion from this observation was used then to create a numerical model of the joint (acceptance of an elasto-plastic material of the sheets).

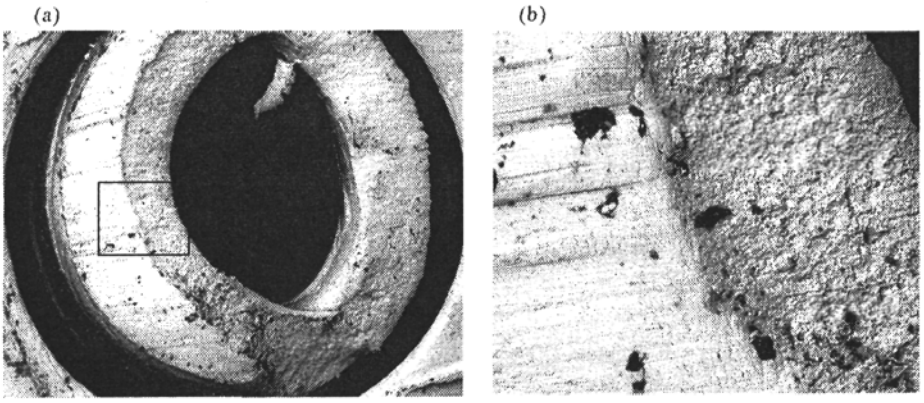

Fig. 16. View of a damaged rivet after a destructive test (JEOL scanning microscope)

5. Numerical fatigue life analysis of the riveted lap joint

To estimate the total fatigue life of the joint, the program MSC Fatigue ver. 9.0 was used. This program enables one to perform two main kinds of analyses: the total fatigue life analysis (S-N) and crack initiation analysis

(ε-N) for non-limited geometry defined by the user (15). In the next part of this study, the S-N analysis was applied to estimate the total fatigue life of the joint loaded by an oscillating force.

The program Fatigue needs the results obtained from the static (linear or nonlinear) analysis as the input data. Mostly, it is a file which contains the maximum principal stress for all nodes of the numerical model. Moreover, the history of the variable load and also fatigue properties of the material must be defined based on the results of experimental standard S-N or ε-N fatigue tests. As a result of the S-N analysis, the number of cycles to total damage of the structure can be obtained. The S-N analysis gives correct results only for high cycle fatigue, when the number of cycles is more than 10^4-10^5.

During the analysis, the program MSC Fatigue uses procedures of "rain flow counting" and "linear damage summation" to transpose the time history used in computation (Fig. 17) on the results of experimental tests performed on standard specimens. In the S-N analysis presented here, the correction of mean stress according to Goodman's theory was additionally applied.

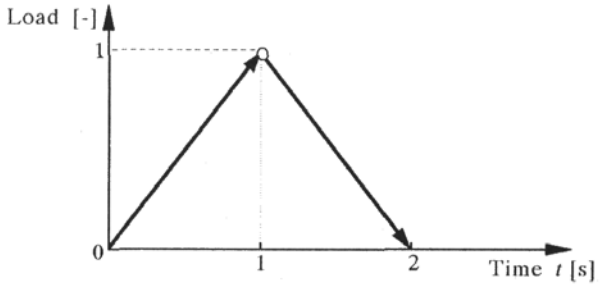

Fig. 17. The load time history used in numerical fatigue life analysis of the riveted joint

The analysis for the cyclic loads with levels of the maximum force between 10% (70 N) and 50% (350 N) of limiting load was performed.

Results of the S-N analysis performed for the rivet (a) and sheets (b) are shown in Fig. 18. The estimated total fatigue life of the rivet for the cyclic load with the maximum level of 350 N is $10^{2.39}$ cycles. Adequately, the fatigue life of sheets for the same load condition is $10^{10.45}$ cycles. The obtained results for different levels of cyclic load were systematized and shown in Fig. 19. The fatigue life for both the rivet and sheets for a variable load of 70 N was estimated as 10^{14} cycles. At increasing of the load, the fatigue life of the rivet decreases more than the life of sheets.

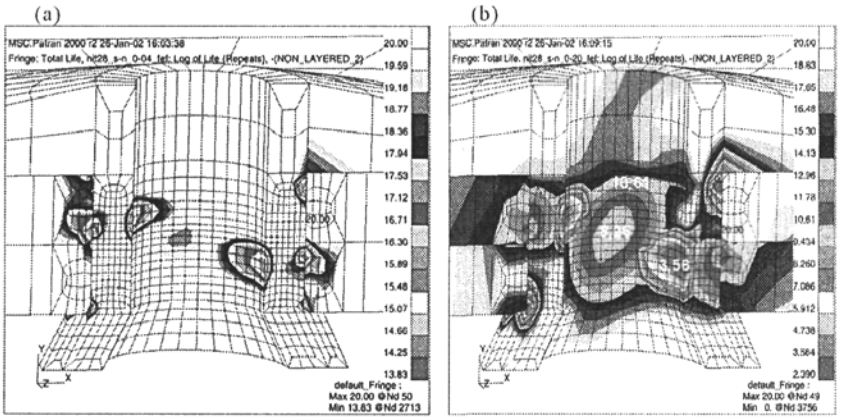

Fig. 18. Results of the S-N analysis (zones of the FE model with determined the total fatigue life) for the rivet (a) and sheets (b) for variable load with the maximum level of 350 N

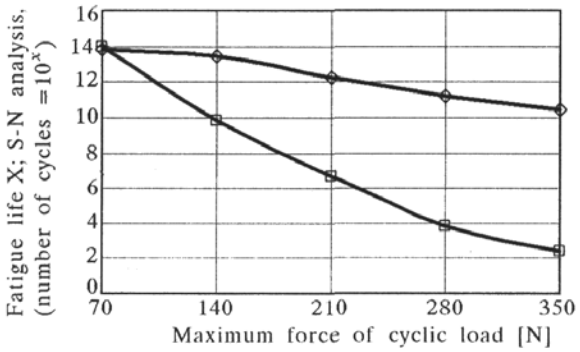

Fig. 19. A plot of the total fatigue life of joint components: the rivet and sheets in function of cyclic loads with different levels of the maximum force

6. Conclusions

This paper presents results of complex static and fatigue calculations and experimental investigations of a lap blind riveted joint. To solve the problem, multi-step numerical analysis concerning respectively the riveting and the shearing process was carried out. In the first analysis, the initial stress state formed in the riveting process was obtained. Next, the riveted joint with defined initial stresses was subjected to shear. The obtained results (load-displacement characteristic and limited load capacity) were then validated by an experimental test. Their interpretation made it possible to understand better the phenomena occurring during the riveting or shearing process of riveted joints.

The following remarks can be formulated based on the numerical and experimental results carried out through out the work:

- In terms of fatigue, highly loaded riveted joints must have a denser pith of the joint than the width of sheets considered in this analysis. For a cyclic load with the maximum level of 350 N (50% limiting load), the fatigue life of sheets estimated numerically way (Fig. 19) is larger than the life of the rivet. For smaller cyclic loads, the required pith of the riveted joint can be thinner. The procedure presented in the paper can by useful for design of different structures with programmable fatigue life.

- On the base of numerical calculations performed for models with different numbers of elements, very similar results were found. The fluctuation of the limiting load capacity was only 8% for completely different sizes of numerical tasks in models with 2916 and 7664 elements. For different numerical problems such as stress or stability analysis, the influence of the total number of finite elements is more significant.

- In the numerical analysis of riveted joints, some problems with the definition of certain parameters such as the actual friction coefficient of adjacent sheets, real yield point and tensile strength of the alloy used for manufacturing of a rivet occur. The strength parameters taken from standards have certain fluctuations and, moreover, depend on the heat treatment state.

  For this reason, divergence between a numerical model and a real structure of a joint can be observed.

References

1. AL-EMRANI M., KLIGER R., 2003, FE analysis of stringer-to-floor-beam connections in riveted railway bridges, *Journal of Constructional Steel Research*, **59**, 803-818
2. DENG X., HUTCHINSON J.W., 1998, The clamping stress in a cold-driven rivet, *Int. J. Mech. Sci*, **40**, 7, 683-694
3. DIBATTISTA J., ADAMSON D., KULAK G., 1998, Fatigue strength of riveted connections, *Journal of Structural Engineering*, **24**, 7, 792-797
4. FITZGERALD T.J., COHEN J.B., 1994, Residual stresses in and around rivets in clad aluminium alloy plates, *Material Science and Engineering*, **A188**, 51-58

5. FUNG C-P., SMART J., 1997, Riveted single lap joints. Part 1: numerical parametric study, *Proc. Instn. Mech. Engrs*, **211**, part G, 13-27

6. GALATOLO R., NILLSON K.-F., 2001, An experimental and numerical analysis of residual strength of butt-joints panels with multiple site damage, *Engineering Fracture Mechanics*, **68**, 1437-1461

7. KARAOGLU C., KURALAY N.S., 2002, Stress analysis of a truck chasis with riveted joints, *Finite Elements in Analysis and Design*, **38**, 1115-1130

8. KELLY B., COSTELLO B., 2004, FEA modelling of setting and mechanical testing of aluminum blind rivets, *Journal of Materials Processing Technology*, **153**, 74-79

9. LANGRAND B., DELETOMBE E., MARKIEWICZ E., DRAZETIC P., 1999, Numerical approach for assessment of dynamic strength for riveted joints, *Aerospace Science and Technology*, **3**, 431-466

10. LANGRAND B., DELETOMBE E., MARKIEWICZ E., DRAZETIC P., 2001, Riveted joints modeling for numerical analysis of airframe crashworthiness, *Finite Elements in Analysis and Design*, **38**, 21-44

11. LANGRAND B., PATRONELLI L., DELETOMBE E., MARKIEWICZ E., DRAZETIC P., 2002, An alternative numerical approach for full scale characterisation for riveted joints, *Aerospace Science and Technology*, **6**, 343-354

12. LIAO M., SHI G., XIONG Y., 2001, Analytical methodology for predicting fatigue life distribution of fuselage splices, *International Journal of Fatigue*, **23**, 177-185

13. LIU L., SAWA T., 2001, Stress analysis and strength evaluation of single-lap adhesive joints combined with rivets under external bending moments, *Journal of Adhesion in Science and Technology*, **15**, 1, 43-61

14. LUCAS F.M., SILVA, J.P, GONALVES, F. OLIVEIRA, P., 2000, Multiple-site damage in riveted lap-joints: experimental simulationand finite element prediction, *International Journal of Fatigue*, **22**, 319-338

15. MSC Fatigue 9.0, *Quick Start Guide*, Los Angeles

16. MSC/Patran Advanced FEA - *User's manual - Modeling and analysis guidelines*

17. NEVES L., CRUZ P., HENRIQUES A., 2001, Reliability analysis of steel connection components based on FEM, *Engineering Failure Analysis*, **8**, 29-48

18. RAKOWSKI G., KACPRZYK Z., 1993, *Metoda elementów skończonych w mechanice konstrukcji*, Oficyna Wydawnicza Politechniki Warszawskiej

19. SKRZYPEK J., 1986, *Plastyczność i pełzanie*, PWN Warszawa

20. TERADA H., 2001, Structural fatigue and joint degradation, *International Journal of Fatigue*, **23**, 21-30

21. URBAN M.R., 2003, Analysis of the fatigue life of riveted sheet metal helicopter airframe joints, *International Journal of Fatigue*, **25**, 1013-1026

22. WITEK L., 2000, Numerical-experimental analysis of the limiting load of riveted joints, (in Polish), *Proceedings of the 5-th National Conference of FEM Programs users (MSC)*, Warszawa-Rynia, Poland, 243-251

23. WITEK L., 2001, Numerical analysis of the initial stress forming in the process of blind riveting, *Proceedings of 7-th International Conference TECHNOLOGIA 2001*; Bratysława, Slowakia, **2**, 736-739

24. WITEK L., 2002, Numerical-experimental analysis of stability and limiting load of cylindrical shell reinforced by stringers in the shape of closed formers subjected to torsion, (in Polish), doctor's thesis, Rzeszow University of Technology, Faculty of Mechanical Engineering and Aeronautics, Rzeszow, Poland

25. WITEK L., KOPECKI T., MAZUREK P., 1999, The problem of load capacity and stress distribution of thin-walled sheet duraluminium adhesived-riveted joints, *Proceedings of the 4-th International Scientific Colloquium CAX TECHNIQUES*, Bielefeld, Germany, 73-78

26. XIONG Y., 1999, Analytical and finite element modeling of riveted lap joins in aircraft structure, *AIAA Journal*, **37**, 93

Numeryczno-eksperymentalna analiza naprężeń wstępnych, nośności granicznej oraz trwałości zmęczeniowej połączeń nitowych

Streszczenie

Praca przedstawia wyniki obliczeń numerycznych oraz badań eksperymentalnych dotyczących zakładkowego połączenia nitowego z wykorzystaniem tzw. nitów zrywalnych. W pracy dokonano analizy procesu zakuwania nita oraz wyznaczono wielkość naprężeń wstępnych powstających w procesie zakuwania. Następnie analizowano procesy zachodzące w trakcie ścinania połączenia (z uwzględnieniem naprężeń wstępnych powstałych w procesie nitowania). Uzyskano szereg wyników, m.in. numeryczną charakterystykę ścinania połączenia nitowego oraz zależność nośności granicznej w funkcji liczby elementów modelu. Uzyskane wyniki zostały następnie zweryfikowane eksperymentalnie. W ostatniej części pracy analizowano na drodze numerycznej wpływ wielkości obciążenia zmiennego na trwałość zmęczeniową połączenia nitowego.

Manuscript received November 22, 2004; accepted for print February 10, 2005